Available online at www.sciencedirect.com

SciVerse ScienceDirect

Ceramics International 39 (2013) 4651–4656

CERAMICS INTERNATIONAL

www.elsevier.com/locate/ceramint

Short communication

Study on visible light response and magnetism of bismuth ferrites synthesized by a low temperature hydrothermal method

Yuxia Sun[a], Xiangyu Xiong[b], Zhao Xia[b], Hongri Liu[b,c,*], Yong Zhou[b], Man Luo[b], Chengyan Wang[b]

[a]College of Computer Science and Technology, Hubei Normal University, Huangshi 435002, China
[b]College of Physics and Electronic Science, Hubei Normal University, Huangshi 435002, China
[c]Hubei Key Laboratory of Pollutant Analysis and Reuse Technology, Huangshi 435002, China

Received 8 August 2012; received in revised form 15 October 2012; accepted 16 October 2012
Available online 31 October 2012

Abstract

$BiFeO_3$ and $Bi_{25}FeO_{40}$ microspheres were synthesized via a hydrothermal process and their structure, visible light response, and magnetism were investigated. Pure $BiFeO_3$ and $Bi_{25}FeO_{40}$ powders were obtained at 120 °C and 100 °C, respectively. Both of the $Bi_{25}FeO_{40}$ and $BiFeO_3$ powders exhibited strong absorption in visible-light regime. Antiferromagnetism and super-paramagnetism were observed in $BiFeO_3$ and $Bi_{25}FeO_{40}$ respectively.

Keywords: Bismuth ferrites; Hydrothermal method; Optical band gap; Magnetism

1. Introduction

Bismuth ferrites have attracted much interest due to their physical properties and extensive application potentials [1,2]. It is a large family that includes perovskite, garnet and sillenite structural compounds in which the sillenite exhibits various properties such as photorefractivity, optical activity and photoconductivity and these properties have application potentials in electro-optics, acoustics, and piezotechnics [3,4]. Perovskite-structural $BiFeO_3$ (BFO) shows the coexistence of ferroelectric and magnetic orders at room temperature; therefore, it is known as a type of typical multiferroic material. The Curie temperature of BFO is 830 °C and the Neel temperature is 370 °C [5]. It is a rhombohedrally distorted perovskite structure belonging to the space group R3c. The multiferroic behavior presents not only opportunities for the study of fundamental physics but also potential applications in information storage, spintronics, and sensors [6,7]. Recently, BFO is reported to display distinct photovoltaic effect and a 0.8–0.9 V open circuit voltage in a working solar device, which added a new application potential to it [8,9].

The synthesis technique and process are crucial to the microstructure of bismuth ferrites, thus determining the physical properties of products. Various techniques have been developed to synthesize bismuth ferrites, such as the co-precipitation method [10], soft chemical route [11], the molten-salt method, the sol–gel process, etc. [12,13]. All of the above methods need a sintering process at high temperature (>400 °C), thus being energy consuming. The hydrothermal process is a type of powerful method for the fabrication of anisotropic powders because of its great chemical flexibility and synthetic tenability. It possesses advantages such as low process temperature, energy saving, good dispersion, small particle size, etc. [14,15]. However, most sillenite crystals have been grown by the standard Czochralski method or by the liquid-phase epitaxy method [16,17] and there are relatively few reports on the synthesis of $Bi_{25}FeO_{40}$ crystal by the hydrothermal method. Meanwhile, although the hydrothermal method is commonly used to prepare perovskite-structural BFO, it is difficult to obtain

*Corresponding author at: College of Physics and Electronic Science, Hubei Normal University, Cihu Road No. 11, Huangshi 435002, China.
E-mail address: lhr1229@126.com (H. Liu).

0272-8842/$ - see front matter © 2012 Elsevier Ltd and Techna Group S.r.l. All rights reserved.
http://dx.doi.org/10.1016/j.ceramint.2012.10.212

pure perovskite phase under low temperature. To the best of our knowledge, the lowest reaction temperature to obtain pure BFO by the hydrothermal method is 130 °C. Under such a reaction temperature, BFO was acquired with the aid of triethanolamine and the shape of the particle is irregular [18]. Therefore, the exploration of a hydrothermal route to synthesize bismuth ferrites at lower reaction temperature with controllable microstructure is an important work.

In the present work, we report the hydrothermal synthesis method of bismuth ferrites with different morphologies. Well-defined $Bi_{25}FeO_{40}$ and $BiFeO_3$ microspheres have been obtained by controlling reaction temperature. We obtained pure $Bi_{25}FeO_{40}$ and $BiFeO_3$ microspheres at 100 °C and 120 °C respectively using $Bi(NO_3)_3 \cdot 5H_2O$ and $Fe(NO_3)_3 \cdot 9H_2O$ as starting materials and distinct magnetism was observed. Our work supplies an effective hydrothermal synthesis route to obtain pure bismuth ferrites under low temperature.

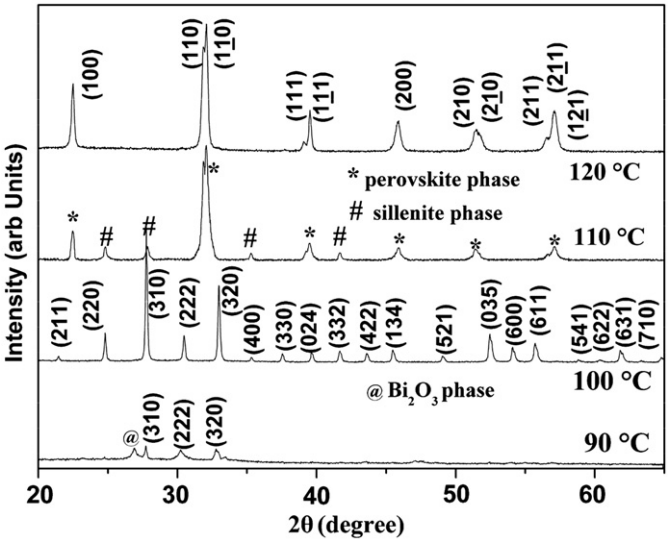

Fig. 1. XRD patterns of bismuth ferrites.

2. Experimental

The bismuth ferrites were prepared by the hydrothermal synthesis method. $Fe(NO_3)_3 \cdot 9H_2O$ and $Bi(NO_3)_3 \cdot 5H_2O$ were dissolved in 20 mL 2-methoxyethanol to obtain transparent solution by constant stirring. Then 5 mL ethanolamine was added into the above solution as slowly as possible to precipitate Bi^{3+} and Fe^{3+}. The precipitate was washed with distilled water repeatedly to remove solvent and other organic components. After filtering, the precipitate was mixed with 12 M KOH solution and distributed by ultrasonication for 10 min. Here, KOH was used to adjust pH value and also served as a mineralizer. The above solution was transferred into a Teflon-lined steel autoclave. The autoclave was sealed and then heated at 90 °C, 100 °C, 110 °C or 120 °C for 8 h. The products were collected at the bottom of the autoclave after it was furnace-cooled to room temperature. Finally, the products were washed with distilled water several times, and then dried in air for characterization.

Powder XRD data were collected at 298 K on an X-ray diffractometer (Phillips X-Pert Highscore) with Cu Kα radiation. Micrographs of the samples were taken with a JSM600 SEM (JEOL Japan). TEM images were taken with a 200CX system (JEOL Japan). The absorption spectra were measured using a UV–vis spectrophotometer (Model lambda 35, Perkin-Elmer, Waltham, MA). The magnetism was measured with a physical property measurement system (Quantum Design, San Diego, CA).

3. Results and discussion

Fig. 1 shows the XRD patterns of the bismuth ferrites powders synthesized by the low temperature hydrothermal method reacting at 90 °C, 100 °C, 110 °C and 120 °C. As shown in Fig. 1, the XRD pattern of the bismuth ferrites synthesized at 90 °C can be indexed to a composite with the coexistence of Bi_2O_3 and $Bi_{25}FeO_{40}$. When the reaction temperature increases to 100 °C, the XRD pattern can be indexed to $Bi_{25}FeO_{40}$ sillenite phase with a cubic structure belonging to I23 space group (ICSD: 041937) and there are no peaks from impurity can be spotted. A composite composed of $Bi_{25}FeO_{40}$ and BFO can be identified according to the XRD pattern of the sample obtained at 110 °C. For the sample reacting at 120 °C, pure perovskite phase with a rhombohedrally distorted structure belonging to R3m space group can be observed, well consistent with the reported data (ICSD: 020372) and no peaks from impurity can be observed. Therefore we can confirm that it is pure $BiFeO_3$.

The morphologies of the bismuth ferrites synthesized at 90 °C (BFO1), 100 °C (BFO2), 110 °C (BFO3) and 120 °C (BFO4) were examined using scanning electron microscopes. As shown in Fig. 2(a) and (b), the BFO1 powders are composed of nanoparticles of 300 nm. The sample BFO2 exhibits well-defined microsphere morphology and the diameter is about 16 μm. The morphologies of BFO3 and BFO4 are shown in Fig. 3. It can be seen from Fig. 3(a) that the BFO3 powders are composed of irregular fractions and microspheres of 12 μm. Fig. 3(b) shows that the microspheres are composed of nanoparticles of 200 nm. As shown in Fig. 3(c), the BFO4 is composed of well defined microspheres of 50 μm. The SEM result of higher magnification showed that the BFO4 microspheres exhibit incompact structure and are composed of particles with the size of several hundreds of nanometers (shown in Fig. 3(d)).

We examined the two pure samples BFO2 and BFO4 with TEM further to confirm the morphology and size of the component particles. Before measuring, the two samples were distributed in absolute alcohol by ultrasonication for 5 min. Fig. 4(a) shows the typical TEM images of the BFO4. We can see that the BFO4 microspheres are composed of uniform and nearly cubical nanoparticles with a size

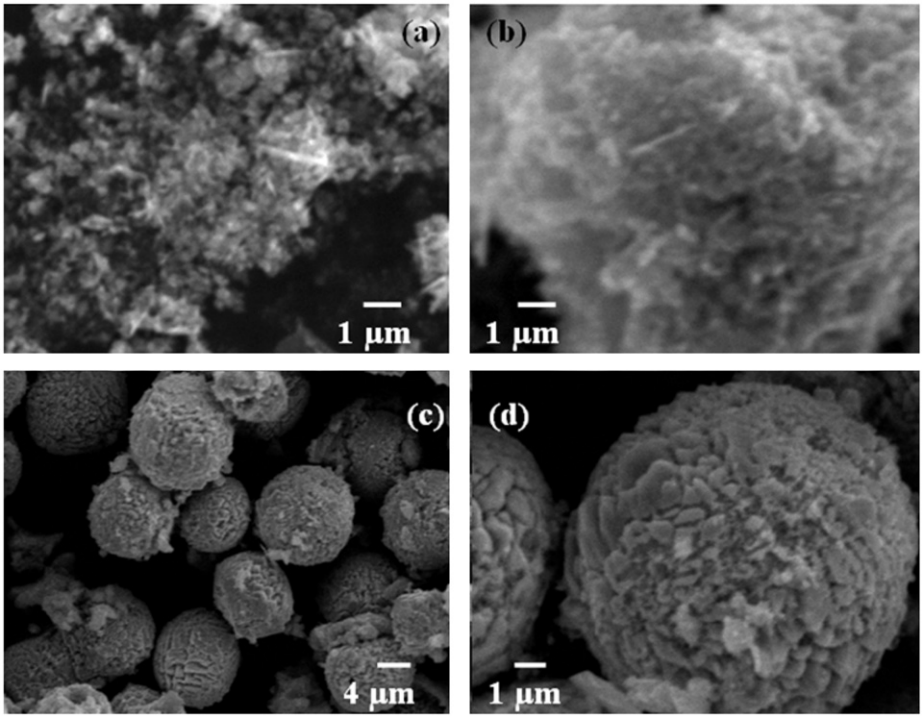

Fig. 2. SEM photos of bismuth ferrites: (a) and (b) reacted at 90 °C and (c) and (d) reacted at 100 °C.

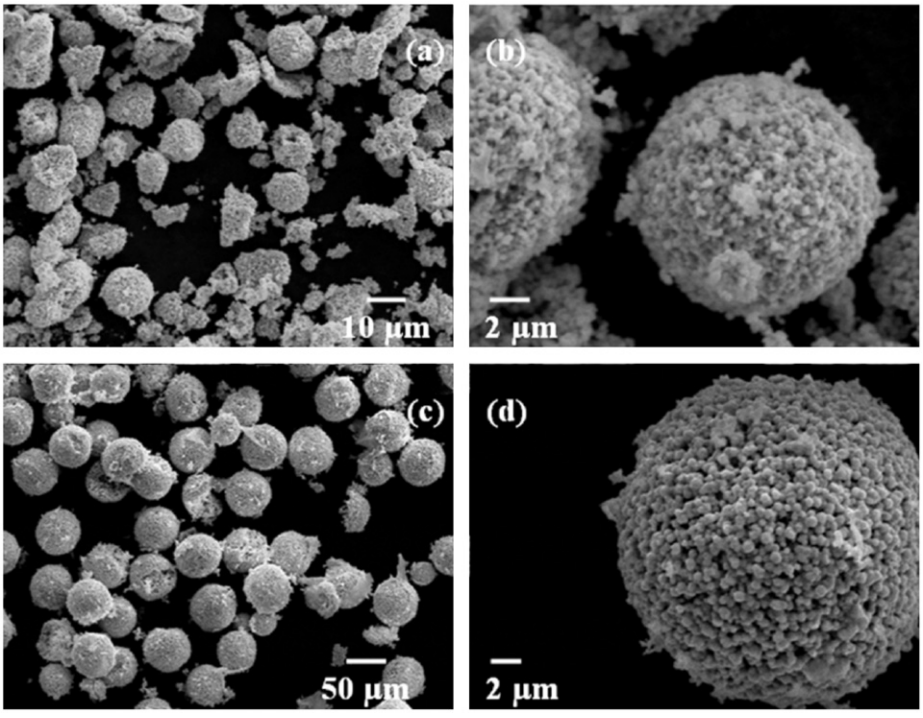

Fig. 3. SEM photos of bismuth ferrites: (a) and (b) reacted at 110 °C and (c) and (d) reacted at 120 °C.

of 200 nm. The result is similar to the $BiFeO_3$ nanocubes synthesized at 180 °C with the microwave hydrothermal method [19]. As for the BFO2, we can see from Fig. 3(b) that it is composed of nanoflakes with a size of 20 nm.

The formation processes of bismuth ferrites in the hydrothermal system can be assigned to two stages. First, $Bi(OH)_3$ and $Fe(OH)_3$ dissolved at low temperature and high pressure were acted upon by a mineralizer (KOH).

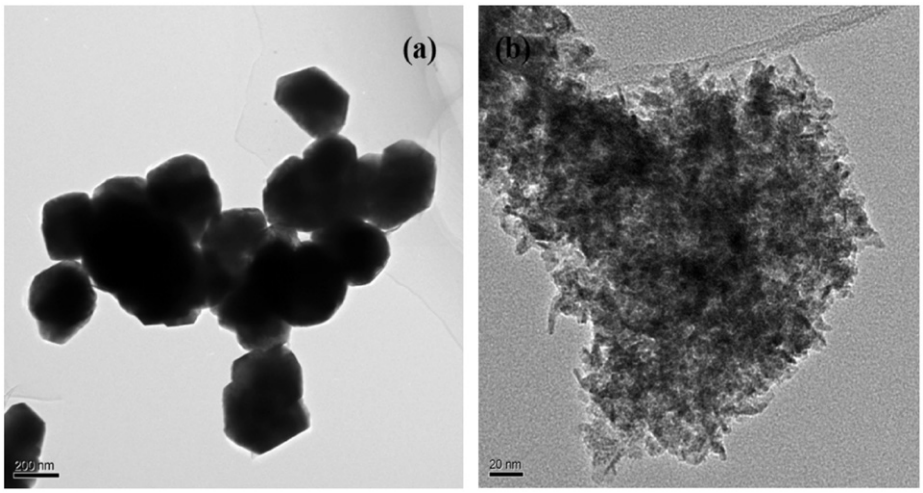

Fig. 4. TEM photos of bismuth ferrites: (a) $BiFeO_3$ and (b) $Bi_{25}FeO_{40}$.

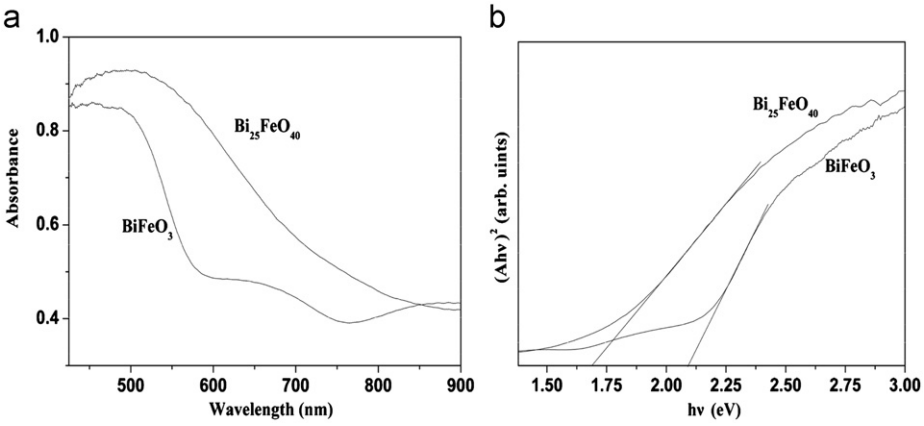

Fig. 5. UV–vis spectroscopies of $BiFeO_3$ and $Bi_{25}FeO_{40}$.

Second, insoluble bismuth ferrites powders precipitated from supersaturated hydrothermal fluid conditions [20]. In the second stage, a large amount of bismuth ferrites crystallites nucleate and grow into small seed crystal particles in the supersaturated solution. As the reaction continued, the small seed crystal particles grow into final bismuth ferrites particles. At 90 °C, $Bi(OH)_3$ and $Fe(OH)_3$ cannot react completely to produce $Bi_{25}FeO_{40}$ because of low temperature; therefore we can observe Bi_2O_3 in the product. At 100 °C, the thermodynamic mechanism is in favor of the formation of $Bi_{25}FeO_{40}$ and we can obtain pure $Bi_{25}FeO_{40}$; when the reaction temperature increases to 110 °C, $BiFeO_3$ phase begins to be generated and we can observe $Bi_{25}FeO_{40}$ and $BiFeO_3$ in the product while at 120 °C, the thermodynamic mechanism is in favor of the formation of $BiFeO_3$; therefore we can obtain pure BFO. Since the reaction temperature of 100 °C is too low, the crystal nucleate of BFO2 cannot grow fully during the reaction process, so we can obtain nanoflakes of only 20 nm finally. At 120 °C, the crystal nucleate of $BiFeO_3$ can grow fully; therefore larger nanoparticles of 200 nm can be acquired. As mentioned above, the lowest reaction temperature to acquire pure $BiFeO_3$ by the hydrothermal method is 130 °C [19] and the size of BFO nanoparticles is not even; therefore, our work supplies an effective route to obtain uniform BFO nanoparticles under very low temperature.

Because BFO2 ($Bi_{25}FeO_{40}$) and BFO4 ($BiFeO_3$) exhibit pure sillenite structure and perovskite structure, respectively, we studied their UV–vis absorption property and magnetism. Fig. 5 shows the UV–vis absorption spectroscopy of the BFO2 and BFO4 powders. As can be seen in Fig. 5(a), the absorption spectrum of BFO4 shows a sharp increase at approximately 500 nm, along with two slight absorption tails at 650 and 870 nm, suggesting that $BiFeO_3$ powders can absorb remarkable amounts of visible light. The absorption spectrum of BFO2 shows smooth increase at approximately 500 nm and ends at 900 nm. This means that BFO2 powders have a wider absorption range to visible light than that of BFO4. The optical band gaps of the bismuth ferrites powders are shown in Fig. 5(b). The calculated value of BFO from the absorption spectrum is

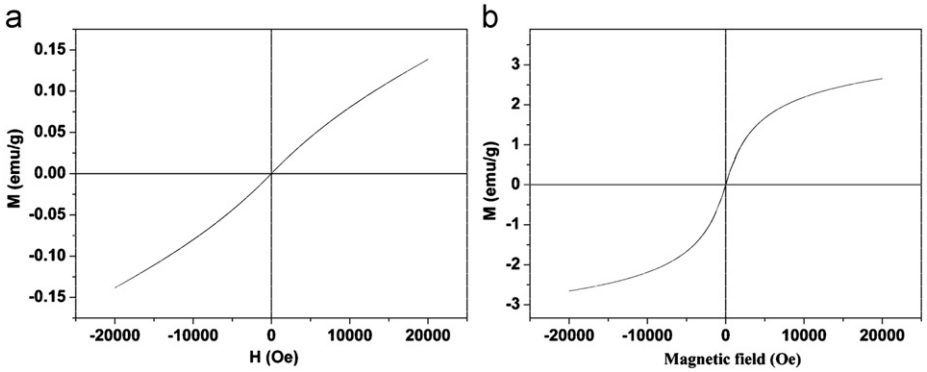

Fig. 6. *M–H* curves of bismuth ferrites: (a) $BiFeO_3$ and (b) $Bi_{25}FeO_{40}$.

2.09 eV, which is smaller than the result reported by Gao et al. [8] and Chin et al. [18] and larger than the results of BFO pills and rods [21]. For BFO2, the calculated value from the absorption spectrum is 1.68 eV; the result is smaller than the reported results [22]. From the viewpoint of utilizing solar energy as in the applications of photocatalyst and optoelectric devices, the above results suggest that $Bi_{25}FeO_{40}$ powder may have a greater advantage than does $BiFeO_3$ in visible light wave band.

The magnetism of the BFO4 and BFO2 microspheres was also investigated in this paper. As shown in Fig. 6(a), the magnetic hysteresis loop of $BiFeO_3$ showed almost linear field dependence, similar to the report in [22]; it clearly demonstrated that the sample exhibited an antiferromagnetic order at room temperature. According to Fig. 6(b), the antiferromagnetic order came from the superexchange interactions between the iron ions. The magnetic hysteresis loop of $Bi_{25}FeO_{40}$ shows good saturation, and the coercivity and remanent magnetism are nearly zero, revealing super-paramagnetism at room temperature. There are very few reports on the magnetism of $Bi_{25}FeO_{40}$ now. Chen et al. observed paramagnetism in $Bi_{25}FeO_{40}$ under a low applied field. Our result is very similar to the result reported by Tan et al. [22]. More detailed investigations on the magnetic properties of $Bi_{25}FeO_{40}$ are underway. We can also see that under the same maximum applied field, the magnetization of $Bi_{25}FeO_{40}$ (2.6 emu/g) is of a magnitude order larger than that of $BiFeO_3$ (0.13 emu/g); meanwhile the hysteresis loop of $Bi_{25}FeO_{40}$ shows better saturation than that of $BiFeO_3$. Therefore it may have a greater advantage than does $BiFeO_3$ in the applications of magnetism.

4. Conclusion

In conclusion, pure $BiFeO_3$ and $Bi_{25}FeO_{40}$ microspheres were synthesized via a hydrothermal process at low temperatures of 120 °C and 100 °C respectively. The uniform $BiFeO_3$ microspheres consisted of very uniform nanocubes of 200 nm and the $Bi_{25}FeO_{40}$ microspheres were composed of nanoflakes of 20 nm. The optical band gaps of $BiFeO_3$ and $Bi_{25}FeO_{40}$ are 2.09 eV and 1.68 eV, respectively. Under a maximum applied magnetism field, the $BiFeO_3$ and $Bi_{25}FeO_{40}$ show antiferromagnetism and super-paramagnetism respectively. The $Bi_{25}FeO_{40}$ showed advantages in magnetism and optical properties compared to the $BiFeO_3$. The present work supplies an effective route to prepare bismuth ferrites by the hydrothermal method under very low temperatures.

Acknowledgments

The work is supported by the Key Program of Hubei Province Education Committee under Grant no. D201222006.

References

[1] Y. Chen, Q. Wu, J. Zhao, Selective synthesis on structures and morphologies of $Bi_xFe_yO_z$ nanomaterials with disparate magnetism through time control, Journal of Alloys and Compounds 487 (2009) 599–604.
[2] K.Y. Yun, M. Noda, M. Okuyama, Prominent ferroelectricity of $BiFeO_3$ thin films prepared by pulsed-laser deposition, Applied Physics Letters 83 (398) (2003) 1–3.
[3] M. Zaleski, Thermally stimulated processes related to photochromism of scandium doped sillenites, Journal of Applied Physics 87 (2000) 4279–4284.
[4] E. Nippolainen, A.A. Kamshilin, V.V. Prokofiev, T. Jaaskelainen, Combined formation of a self-pumped phase-conjugate mirror and spatial subharmonics in photorefractive sillenites, Applied Physics Letters 78 (2001) 859–861.
[5] J. Wang, J.B. Neaton, H. Zheng, et al., Epitaxial $BiFeO_3$ multiferroic thin film heterostructures, Science 299 (2003) 1719–1722.
[6] Z.X. Cheng, X.L. Wang, H. Kimura, K. Ozawa, S.X. Dou, La and Nb codoped $BiFeO_3$ multiferroic thin films on $LaNiO_3$/Si and IrO_2/Si substrates, Applied Physics Letters 92 (2008) 092902-1–3.
[7] S.T. Zhang, M.H. Lu, D. Wu, Y.F. Chen, N.B. Ming, Larger polarization and weak ferromagnetism in quenched $BiFeO_3$ ceramics with a distorted rhombohedral crystal structure, Applied Physics Letters 87 (2005) 262907-1–3.
[8] F. Gao, X. Chen, K. Yin, S. Dong, Z. Ren, F. Yuan, T. Yu, Z. Zou, J. Liu, Visible-light photocatalytic properties of weak magnetic $BiFeO_3$ nanoparticles, Advanced Materials 19 (2007) 2889–2892.
[9] S.Y. Yang, L.W. Martin, S.J. Byrnes, T.E. Conry, et al., Photovoltaic effects in $BiFeO_3$, Applied Physics Letters 95 (2009) 062909-1–3.

[10] S. Shetty, V.R. Palkar, R. Pinto, Size effect study in magnetoelectric $BiFeO_3$ system, Pramana—Journal of Physics 58 (2002) 1027–1030.
[11] S. Ghosh, S. Dasgupta, A. Sen, H.S. Maiti, Low-temperature synthesis of nanosized bismuth ferrite by soft chemical route, Journal of the American Ceramic Society 88 (2005) 1349–1352.
[12] X. He, L. Gao, Synthesis of pure phase $BiFeO_3$ powders in molten alkali metal nitrates, Ceramics International 35 (2009) 975–978.
[13] T. Liu, Y. Xu, J. Zhao, Low-temperature synthesis of $BiFeO_3$ via PVA sol–gel route, Journal of the American Ceramic Society 93 (2010) 3637–3641.
[14] G. Biasotto, A.Z. Simões, C.R. Foschini, M.A. Zaghete, J.A. Varela, E. Longo, Microwave-hydrothermal synthesis of perovskite bismuth ferrite nanoparticles, Materials Research Bulletin 46 (2011) 2543–2547.
[15] H. Zhang, K. Kajiyoshi, Hydrothermal synthesis and size-dependent properties of multiferroic bismuth ferrite crystallites, Journal of the American Ceramic Society 93 (2010) 3842–3849.
[16] H. Marquet, M. Tapiero, J.C. Merle, J.P. Zielinger, J.C. Launay, Determination of the factors controlling the optical background absorption in nominally undoped and doped sillenites, Optical Materials 11 (1998) 53–65.
[17] A.V. Egorysheva, V.V. Volkov, V.I. Burkov, T.D. Dudkina, Y.F. Kargin, Growth and characterization of bismuth borate crystals, Optical Materials 13 (1999) 361–365.
[18] M.C. Chin, H.N. Jun, I.S. Cho, J.S. An, K.S. Hong, Low-temperature hydrothermal synthesis of pure $BiFeO_3$ nanopowders using triethanolamine and their applications as visible-light photocatalysts, Journal of the American Ceramic Society 91 (2008) 3753–3755.
[19] U.A. Joshi, J.S. Jang, P.H. Borse, J.S. Lee, Microwave synthesis of single-crystalline perovskite $BiFeO_3$ nanocubes for photoelectrode and photocatalytic applications, Applied Physics Letters 92 (2008) 242106-1–3.
[20] M. Hojamberdiev, Y. Xu, F. Wang, W. Liu, J. Wang, La-modification of multiferroic $BiFeO_3$ by hydrothermal method at low temperature, Inorganic Materials 45 (2009) 1183–1187.
[21] L. Fei, J. Yuan, Y. Hu, C. Wu, J. Wang, Y. Wang, Visible light responsive perovskite $BiFeO_3$ pills and rods with dominant $\{111\}_c$ facets, Crystal Growth & Design 11 (2011) 1049–1053.
[22] G. Tan, Y. Zheng, H. Miao, A. Xia, H. Ren, Controllable microwave hydrothermal synthesis of bismuth ferrites and photocatalytic characterization, Journal of the American Ceramic Society 95 (2012) 280–289.